Oblique Genomics Mixture of Experts: Prediction of Brain Disorder With Aging-Related Changes of Brain's Structural Connectivity Under Genomic Influences

Yanjun Lyu[1], Jing Zhang[1], Lu Zhang[2], Wei Ruan[3], Tianming Liu[3], and Dajiang Zhu[1], for the Alzheimer's Disease Neuroimaging Initiative *

[1] Department of Computer Science and Engineering, University of Texas at Arlington, Arlington TX 76019, USA
[2] Department of Computer Science, Indiana University Indianapolis, Indianapolis IN 46202, USA
[3] School of Computing, University of Georgia, Athens GA 30602, USA

Abstract. During the process of brain aging, the changes of white matter structural connectivity are closely correlated with the cognitive traits and brain function. Genes have strong controls over this transition of structural connectivity-altering, which influences brain health and may lead to severe dementia disease, e.g., Alzheimer's disease. In this work, we introduce a novel deep-learning diagram, an oblique genomics mixture of experts(OG-MoE), designed to address the prediction of brain disease diagnosis, with awareness of the structural connectivity changes over time, and coupled with the genomics influences. By integrating genomics features into the dynamic gating router system of MoE layers, the model specializes in representing the structural connectivity components in separate parameter spaces. We pretrained the model on the self-regression task of brain connectivity predictions and then implemented multi-task supervised learning on brain disorder predictions and brain aging prediction. Compared to traditional associations analysis, this work provided a new way of discovering the soft but intricate inter-play between brain connectome phenotypes and genomic traits. It revealed the significant divergence of this correlation between the normal brain aging process and neurodegeneration.

Keywords: Structural Connectivity · Mixture of Experts · Genomics · Alzheimer's Disease · Mild Cognitive Impairment

1 Introduction

Both normal brain aging and pathological aging are mysterious processes, in which not only genetic traits play important roles but are subject to accumulative

* Data used in preparation of this article were obtained from the Alzheimer's Disease Neuroimaging Initiative (ADNI) database (adni.loni.usc.edu).

environmental influences [14]. Evidence shows that the normal aging processes are coupled with the changes in the brain's white matter (WM) connectivity characteristics, while the heterogeneous connectivity characteristics adaptations have also been observed throughout neurodegenerative disorders during brain aging[4, 3, 8, 15]. For instance, closely related to the pathological brain aging process, Alzheimer's disease (AD) and its prodromal clinical stage - mild cognitive impairment (MCI) are known as neurodegenerative stages which are concurrent with disruptions and alterations in brain structural connectivity (SC) [10, 17, 13, 19, 1, 26, 28, 22]. In the view of genomics, genome-wide association studies have identified numerous genomic loci which significantly linked to the AD, and there are potential unrevealed causal genes and variants that characterized the disease via diverse pathways[18, 23, 11, 21, 14]. To summarize, the underlying hypothesis is that genomics has strong control over the molecular level connectivity between different brain regions and partially facilitates the corresponding SCs. However, the precise mechanisms governing genomic-SC level regulation and how SC aging relates to AD pathology remain less elucidated. The main challenge rests on how to comprehensively understand the intricate causal and additive relationships in the triad and merge the multimodality data to contribute to the early prediction of brain aging disorders.

An effective way to fuse these diverse modalities is to obliquely incorporate the genomics features into the analysis of structural connectivity. Inspired by sparse MoE architectures[20, 2, 12], this article introduce the oblique genomics MoE(OG-MoE) (Figure 1), a sparse expert variant of the encoder-only transformer architecture that takes the brain's SC features as input. The "Oblique genomics" stands for the unique individual genomic profiles which used to representing the genomics information. The sparse genomic profile features are added to the model stem by a stand-alone gate function, acting as dynamic bias to influence the selection of experts of SC features. The clinical goal of OG-MoE is predicting CN(Normal)/MCI/AD research groups from subjects' SC features with the help of genomic information. During the training, the model uses a multi-task training diagram to predict the diagnosis label and the SC changes label caused by brain aging. This allows the model to detect the divergences in the SC changes caused by the differences between normal aging and pathological aging under a genomics view. In addition to the benefit of efficiency gained by the employment of highly specialized experts, the oblique incorporation of genomic modalities also evades possible harmful interferences by directly concatenating the features from diverse sources.

We summarize our main innovations and contributions as follows:

1. Unlike imaging genetic association analyses, this work takes the imaging modality (SCs) as the main feature and uses genomic profile to control the self-regression of image modality. The approach mitigates the substantial representational disparity and sematic distinction between genomic features and brain-connectivity features, facilitating a flexible integration of the two modalities.

2. The model considered the inputs of multi-visit data from Alzheimer's Disease Neuroimaging Initiative (ADNI) dataset[16]. By construction of the true paired SC sequence data of two age points and the negative counterparts, the model is designed to address two tasks simultaneously: predict clinical research group and SC changes over time. which potentially facilitates the detection of SC alterations of normal brain aging and pathological aging.
3. As the alternation of vanilla MoE structure, OG-MoE improved the sparse experts' framework with a shared expert, which is free from genomic bias to capture the environmental influences on SC features.

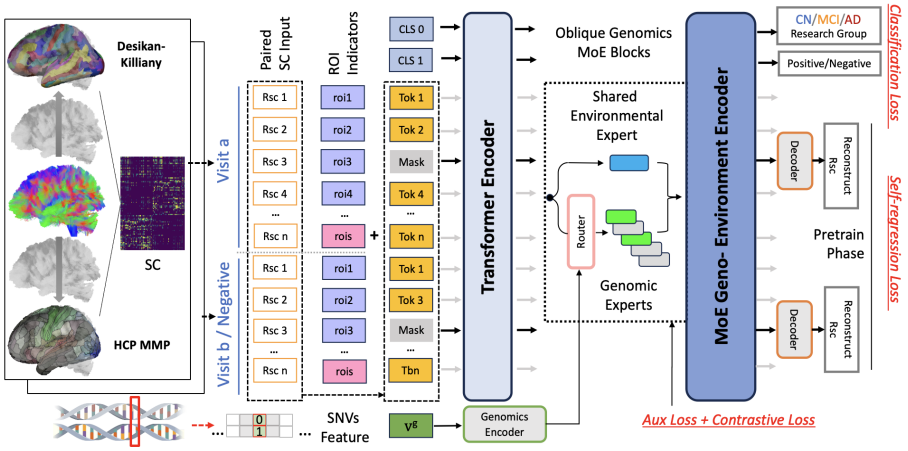

Fig. 1: Framework of the OG-MoE. The model is based on Bert-style transformer encoders and the mixtures of sparse expert diagram with the special gating router, which combines genomics features. The model takes formulated image modality (paired SC sequences) and SNVs features as input. The model is able to learn the normal aging and the neurodegenerative disorders symbols from SC changes with genomic influences.

2 Methodology

2.1 Data Collection and Processing

Data collection In this study, the total number of subjects was 631 (324 females, 307 males; 75.34 ± 7.39 years). Each subject had corresponding genomic records and has no diagnostic group transition between different visits. Within these subjects, 463 individuals have more than one visit, and after a quality check, there is only one DTI image selected for each visit. A total of 1703 diffusion tensor imaging (DTI) MR images were collected. The subjects with multiple

visits and their images (CN: 875, MCI:716, AD:112) on different visits are chosen as the training set (80%) and validation set (20%). The rest of the subjects with a solo visit are set as test data (CN: 103, MCI:51, AD:7).

Imaging data process Here, we utilize the brain's structural connectomes defined by probabilistic tracts using diffusion magnetic resonance imaging data on two prevalent used brain atlases: HCP-MMP [9] with 360 regions (cortical) of interest (ROIs) and the Desikan-Killiany [5] atlas with 78 ROIs (cortical and sub-cortical). First, the standard preprocessing procedures have been applied, similar to Zhang et al. [27], including eddy correction, bias correction, and brain extraction. The preprocessed images were further analyzed using DSI-Studio pipelines [24, 25]. After fiber tracking and registration to the Atlas, the brain's SC was established by estimating the fiber count between the ROIs of the two atlas, as $S \in R^{N \times M}, (N = 78, M = 360)$. Then the *Log*-normalization has been cast to the structural connectivity matrix S.

Genomic data process Genomic data of the candidate subjects are acquired and merged from multiple ADNI research phases. The raw SNVs data have been downloaded and processed by Plink software with the following steps: quality control (QC), high missingness removal, Hardy-Weinberg equilibrium (HWE) filter, and linkage disequilibrium (LD) pruning. The SNVs data from the ADNI dataset across multiple phases have been merged and filtered. The filtered SNVs data are later relocated to the reference genome GRCh38.p14 and combined with gene annotations using genome location, by refering to the NCBI's database. Eventually, 216 important SNVs are found to be closely related to the pre-defined candidate functional genes of brain aging and neurodegeneration to represent the sparse genomics profile(Table 3). The final genomics profile vector is calculated as $g \in R^{2 \times G}, (G = 216)$.

2.2 Model overview

The Oblique Genomics MoE (OG-MoE) adapts the Transformer Encoder architecture similar to Bert [6] and MoE [20]. We innovatively integrate a set of recent deep learning advancements, including: 1) We design a multi-task learning (MTL) framework to enhance the performance of several interrelated tasks by integrating information from subjects' diagnostic labels, age-related alterations in brain SC, and the self-regression patterns inherent in SC features. 2) We constructed paired SC sequence data, either from the paired with true aging relationship or the noisy paired data (Section 2.3), to facilitate the MTL framework. 3) The MoE gating module of the framework incorporated the genomics single nucleotide variants (SNVs) features inside the gating router for the experts' selection of the SC sequence tokens(Section 2.6). 4) The training of the model consists of two parts: the pre-train phase (Section 2.4) and the supervised MTL training phase (Section 2.5).

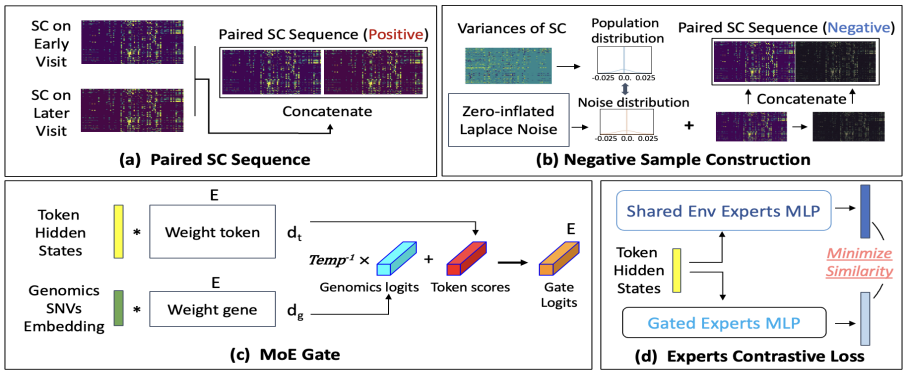

Fig. 2: Detailed design of OG-MOE: (a) paired SC sequence (b) generate negative samples of SC sequence (c) the genomics-guided gating router (d) the contrastive loss of outputs from different experts

2.3 Construction of Paired data

Difference from the traditional model that only focuses on SC data from a single time point. We challenged the OG-MoE model by creating positive and negative paired data. For the positive paired SC sequences, the SC SC^e of a subject's earlier visit and one from the later visit SC^l were concatenated to form a sequence-like input(Fig. 2(a)).

$$Seq^P = \text{concat}(SC^e, SC^l), \quad Seq^P \in R^{2N \times M}, \quad N = 78, M = 360 \tag{1}$$

For the negative paired SC sequences, the later visit SC^l was replaced by the noised SC SC^noise, generated from SC^e. The *Laplace* noise sampling with the zero-inflated method was adopted to mimic the true sparse distribution of the absolute variance between the SC from different visits. (Fig. 2(b))

$$Seq^N = \text{concat}(SC^e, SC^noise), \quad Seq^P \in R^{2N \times M}, \quad N = 78, M = 360 \tag{2}$$

2.4 Self-supervised Pretraining

During this training phase, the paired SC sequences are viewed token-wised on the first dimension, then random masks are applied on the sequence level to the input. The model was optimized to make a reconstruction of those masked tokens at the output, during which the trainable position embedding parameters were added to the SC sequences. This trainable position embedding acts as the ROI indicator (Fig. 1). With SC sequence denoted as Seq, genomics vectors denoted as V^g, and mask indicator m_i, this process can be listed as:

$$Seq' \;=\; (\,x'_1,\; x'_2,\; \ldots,\; x'_N\,), \quad x'_i \;=\; \begin{cases} [\text{MASK}], & \text{if } m_i = 1, \\ x_i, & \text{if } m_i = 0. \end{cases} \tag{3}$$

$$z'_l = MLP(\text{MSA}\big(\text{LN}(z_{l-1}; mask^{Att})\big) \;+\; z_{l-1}), \quad \ell = 1, \ldots, l^k \tag{4}$$

$$z'_j = GMoE((\text{MSA}\big(\text{LN}(z'_j)\big) \;+\; z_{j-1})); v^g), \quad j = l^k, \ldots, L \tag{5}$$

$$\mathcal{L}_{\text{MSE}} \;=\; \sum \Big\| x_i \;-\; D_\theta(z_t) \Big\|^2 \tag{6}$$

Where the MSA, LN, MLP, $GMoE$, D_θ stand for the multi-head attention layers, Layer-norm, MLP layers, genomic MoE layers, and decoder layers respectively. And the $mask^{Att}$ is the causal attention mask added in the multi-head attention layers, to mask out the attention between tokens from the SC sequence of different visits.

2.5 Supervised MTL Training

Based on the pre-trained model, the supervised MTL phase consecutively tuned the model on two tasks. By padding two classification tokens CLS^0 and CLS^1 to the sequence, the model is aimed at predicting the correct research groups (CN/MCI/AD) and positive/negative labels of the constructed SC sequence.

$$y'_{RG} = \text{Linear}\big(CLS^0_L\big), \quad y'_{P/N} = \text{Linear}\big(CLS^1_L\big) \tag{7}$$

$$\mathcal{L}_{cls} = -\lambda_{dual} * KL(y'_{RG}; y_{RG}) + KL(y'_{P/N}; y_{P/N}) \tag{8}$$

2.6 Sparse Mixture of Experts and Oblique Genomics Gating

By revisiting the MoE's gating network (router) mechanisms, we insert the genomic feature vectors into the gating functions as a dynamic bias to influence the scores of the input tokens (Fig. 2(c)). The score logits Z_{logits} can be computed below, $\mathcal{T}$ is the temperature hyperparameter. z^g is logits of the genomic profile vector v^g after the genomic encoder.

$$\mathcal{Z}_{logits} \;=\; w_e^\top z^i_{token} \;+\; \mathcal{T}^{-1} w_g^\top z^g, \quad i = 1, \ldots, N, \tag{9}$$

An additional contrastive loss between the outputs of the shared expert and the outputs of genomics biased routed experts is set to differentiate the function of these two groups of experts. Following the convention of $Penotype = Genomic + Env$, we encourage the shared experts (free from genomics information) to accumulate more environmental feats of SC features (Fig. 2(d)). The z_E and z^i_G are the output of shared experts and i's genomic gated experts, with λ_{cons} as the scale factor.

$$\mathcal{L}_{cons} = \lambda_{cons} * \exp(\text{sim}(z_E, mean(z^i_G))), \quad i = 1, \ldots, N_{experts}, \tag{10}$$

The contrastive loss $\mathcal{L}_{cons}$ and a gate ce-loss of MoE were added into the main model by a compound auxiliary Loss functions during training. The indirect forwards and backward pass algorithm can be formulated as follows.(Algorithm 1)

Algorithm 1 Compound Auxiliary Loss Forward & Backward Pass

Input: x, **Aux Loss**, **Contrastive Loss**
Output: y: identical to x in the forward pass
Forward Pass:
1. **Aux Loss:** Gate CE Loss
2. **Contrastive Loss:** Cosine similarity:$(expertE, expertG)$
3. **Input:** x, Aux Loss, Contrastive Loss
4. **Store** requires_grad ← Aux Loss.requires_grad.
requires_grad ← Contrastive Loss.requires_grad.
5. **Return:** $y = x$

Backward Pass:
1. **Input:** ∇y, the upstream gradient of y (equivalent to ∇x).
2. Initialize ∇Aux Loss $\leftarrow 0$; ∇Contrastive Loss $\leftarrow 0$.
3. Set ∇Aux Loss $= 1; \nabla$Contrastive Loss $= 1$
4. **Return:** ∇y, ∇Aux Loss, ∇Contrastive Loss

3 Experiment

3.1 Model Implementation

The model was empirically set to consist of 19 transformer encoder layers with 8 attention heads and 2 OG-MoE layers to balance the model capacity and computing load. The number of experts was set to 8 and the top 2 experts were set for each token, which achieved the best auxiliary ce-loss during pre-train. The hidden dimension of the model is 128, the temperature $\mathcal{T}$ of OG-MoE gating function to be 0.07, the hyperparameter λ_{dual} to be 0.3, and the hyperparameter $\mathcal{L}_{cons}$ to be 0.05. We employ the Adam optimizer, with a learning rate of 1e-6. The pre-train and supervised training of OG-MoE takes approximately 4 hours on one NVIDIA A6000 GPU.

3.2 Effectiveness of Self-regression Pretraining

The pretraining stage optimized the OG-MoE by mask self-regression learning. The mean squared error metrics of the masked SC vectors and the ground truth were computed and then compared with the mean variance of SC in population data to test the effectiveness of pretraining. The following results show the mean squared error of the predicted masked SC tokens and ground truth in training, validation, and test sets, compared with the variance of SC of the ADNI population (batch size scaled). (Table. 1)

Table 1: Effectiveness of self-regression pretraining of OG-MoE model

Metrics	Train (Batch)	Validation (Batch)	Test (Batch)	SC Var.
MSE	0.007	0.035	0.114	0.598
MSE(CN)	0.006	0.038	0.109	0.594
MSE(MCI)	0.006	0.032	0.127	0.596
MSE(AD)	0.007	0.034	0.102	0.580

3.3 Model Performance

After pretraining, the model was trained on two multi-task scenarios: one was the prediction of CN/MCI with SC pairing labels, and the other one was the prediction of MCI/AD with SC pairing labels. Results were compared with other baseline models.(Table. 2)

Table 2: Results of model performance. "SC": structural connectivity features used in training; "Genomic": genomic features used in training.

Model	Acc.(Avg.)	F1(Avg.)	Acc.(CN/MCI)	Acc.(MCI/AD)
SVM(SC)	0.671	0.581	0.625	0.718
SVM(Genomic)	0.607	0.281	0.546	0.668
Linear(Genomic)	0.318	0.247	0.573	0.623
ViT(SC)[7]	0.693	0.601	0.552	0.804
GO-MoE	<u>0.739</u>	<u>0.701</u>	<u>0.668</u>	<u>0.812</u>

3.4 Experts Selection Pattern

The activation patterns across tasks remain analogous, while the activation patterns on the genomics features and the SC token features show significant differences. However, divergence of the activation patterns of these two kinds of features can be observed between the subsequent classification training (Fig.3).

4 Conclusion

In this work, we propose a novel deep-learning framework, oblique genomics mixture of experts(OG-MoE), designed to predict brain disease diagnoses while accounting for temporal changes in structural connectivity and integrated genomic influences. The model successfully integrated the genomics feature into the imaging modality in brain disease diagnosis prediction. With the innovation added in the MoE diagram and multi-phases and multi-task training strategy, the OG-MoE performs superior to the traditional models and shows strong interpretability.

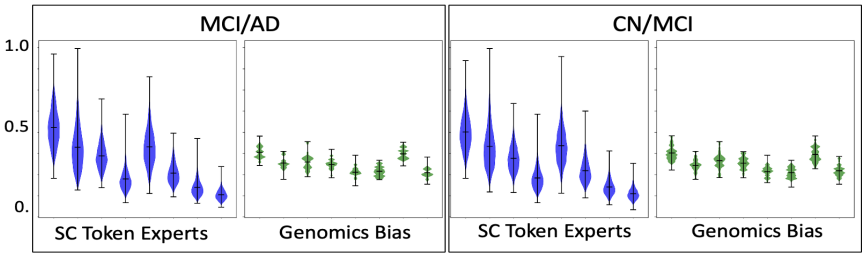

Fig. 3: Difference of SC token experts activation and genomics experts

Table 3: Compose of the genomic profiles: candidate genes symbols and corresponding gene-functions.

Gene Functions	Gene Symbols
Aging	NFE2L2, GPX1, PPARGC1A, TERT, ATG5, SOD2, PARK2, WRN, TPP1, CAT, BLM, IGF1R, DNMT1
Apoptosis	BAK1, TNFRSF10B, TNFRSF10A, FAS, CASP7, TNFRSF1A, BCL2, BID
Sugar Metabolism	SLC2A1, GCK, IGF1, IRS2
Inflammation	S100A8, NLRP3, IL1B, IL1RN, MYD88, TLR2, TNFAIP3, STAT3, TGFB1
Neuron Development	HTT, SNCA, C9orf72, BDNF
AD Critical	CR1, BIN1, SLC4A10, INPP5D, EPHA3, CLNK, HS3ST1, SLC39A8, MEF2C, NME8, SEMA3A, CTTNBP2, CNTNAP2, DPYSL2, PTK2B, NUAK1, MYO16, DAAM1, CCDC88C, SLC24A4, APH1B, MAPT(Tau), CELF4, ALPK2, CASS4, APOE

Acknowledgments. This work was supported by the National Institutes of Health (R01AG075582 and RF1NS128534). Data collection and sharing for this project was funded by the Alzheimer's Disease Neuroimaging Initiative (ADNI)

Disclosure of Interests. The authors have no competing interests to declare that are relevant to the content of this article.

References

1. Catani, M.: Diffusion tensor magnetic resonance imaging tractography in cognitive disorders. Current opinion in neurology **19**(6), 599–606 (2006)
2. Chen, T., Chen, X., Du, X., Rashwan, A., Yang, F., Chen, H., Wang, Z., Li, Y.: Adamv-moe: Adaptive multi-task vision mixture-of-experts. In: Proceedings of the IEEE/CVF International Conference on Computer Vision. pp. 17346–17357 (2023)
3. Coelho, A., Fernandes, H.M., Magalhães, R., Moreira, P.S., Marques, P., Soares, J.M., Amorim, L., Portugal-Nunes, C., Castanho, T., Santos, N.C., et al.: Reorganization of brain structural networks in aging: A longitudinal study. Journal of Neuroscience Research **99**(5), 1354–1376 (2021)

4. Damoiseaux, J.S.: Effects of aging on functional and structural brain connectivity. Neuroimage **160**, 32–40 (2017)
5. Desikan, R.S., Ségonne, F., Fischl, B., Quinn, B.T., Dickerson, B.C., Blacker, D., Buckner, R.L., Dale, A.M., Maguire, R.P., Hyman, B.T., et al.: An automated labeling system for subdividing the human cerebral cortex on mri scans into gyral based regions of interest. Neuroimage **31**(3), 968–980 (2006)
6. Devlin, J., Chang, M.W., Lee, K., Toutanova, K.: Bert: Pre-training of deep bidirectional transformers for language understanding. In: Proceedings of the 2019 conference of the North American chapter of the association for computational linguistics: human language technologies, volume 1 (long and short papers). pp. 4171–4186 (2019)
7. Dosovitskiy, A., Beyer, L., Kolesnikov, A., Weissenborn, D., Zhai, X., Unterthiner, T., Dehghani, M., Minderer, M., Heigold, G., Gelly, S., et al.: An image is worth 16x16 words: Transformers for image recognition at scale. arXiv preprint arXiv:2010.11929 (2020)
8. Fjell, A.M., Walhovd, K.B.: Structural brain changes in aging: courses, causes and cognitive consequences. Reviews in the Neurosciences **21**(3), 187–222 (2010)
9. Glasser, M.F., Coalson, T.S., Robinson, E.C., Hacker, C.D., Harwell, J., Yacoub, E., Ugurbil, K., Andersson, J., Beckmann, C.F., Jenkinson, M., et al.: A multimodal parcellation of human cerebral cortex. Nature **536**(7615), 171–178 (2016)
10. Kim, G.W., Kim, B.C., Park, K.S., Jeong, G.W.: A pilot study of brain morphometry following donepezil treatment in mild cognitive impairment: volume changes of cortical/subcortical regions and hippocampal subfields. Scientific reports **10**(1), 10912 (2020)
11. Lipinski, M.M., Zheng, B., Lu, T., Yan, Z., Py, B.F., Ng, A., Xavier, R.J., Li, C., Yankner, B.A., Scherzer, C.R., et al.: Genome-wide analysis reveals mechanisms modulating autophagy in normal brain aging and in alzheimer's disease. Proceedings of the National Academy of Sciences **107**(32), 14164–14169 (2010)
12. Liu, A., Feng, B., Wang, B., Wang, B., Liu, B., Zhao, C., Dengr, C., Ruan, C., Dai, D., Guo, D., et al.: Deepseek-v2: A strong, economical, and efficient mixture-of-experts language model. arXiv preprint arXiv:2405.04434 (2024)
13. Lo, C.Y., Wang, P.N., Chou, K.H., Wang, J., He, Y., Lin, C.P.: Diffusion tensor tractography reveals abnormal topological organization in structural cortical networks in alzheimer's disease. Journal of Neuroscience **30**(50), 16876–16885 (2010)
14. Lodato, M.A., Walsh, C.A.: Genome aging: somatic mutation in the brain links age-related decline with disease and nominates pathogenic mechanisms. Human molecular genetics **28**(R2), R197–R206 (2019)
15. Park, H.J., Friston, K.: Structural and functional brain networks: from connections to cognition. Science **342**(6158), 1238411 (2013)
16. Petersen, R.C., Aisen, P.S., Beckett, L.A., Donohue, M.C., Gamst, A.C., Harvey, D.J., Jack Jr, C., Jagust, W.J., Shaw, L.M., Toga, A.W., et al.: Alzheimer's disease neuroimaging initiative (adni) clinical characterization. Neurology **74**(3), 201–209 (2010)
17. Qi, S., Meesters, S., Nicolay, K., ter Haar Romeny, B.M., Ossenblok, P.: The influence of construction methodology on structural brain network measures: A review. Journal of neuroscience methods **253**, 170–182 (2015)
18. Schwartzentruber, J., Cooper, S., Liu, J.Z., Barrio-Hernandez, I., Bello, E., Kumasaka, N., Young, A.M., Franklin, R.J., Johnson, T., Estrada, K., et al.: Genome-wide meta-analysis, fine-mapping and integrative prioritization implicate new alzheimer's disease risk genes. Nature genetics **53**(3), 392–402 (2021)

19. Shao, J., Myers, N., Yang, Q., Feng, J., Plant, C., Böhm, C., Förstl, H., Kurz, A., Zimmer, C., Meng, C., et al.: Prediction of alzheimer's disease using individual structural connectivity networks. Neurobiology of aging **33**(12), 2756–2765 (2012)
20. Shazeer, N., Mirhoseini, A., Maziarz, K., Davis, A., Le, Q., Hinton, G., Dean, J.: Outrageously large neural networks: The sparsely-gated mixture-of-experts layer. arXiv preprint arXiv:1701.06538 (2017)
21. Wainberg, M., Forde, N.J., Mansour, S., Kerrebijn, I., Medland, S.E., Hawco, C., Tripathy, S.J.: Genetic architecture of the structural connectome. Nature Communications **15**(1), 1962 (2024)
22. Wang, L., Zhang, L., Zhu, D.: Learning latent structure over deep fusion model of mild cognitive impairment. In: 2020 IEEE 17th International Symposium on Biomedical Imaging (ISBI). pp. 1039–1043. IEEE (2020)
23. Woo, Y.J., Roussos, P., Haroutunian, V., Katsel, P., Gandy, S., Schadt, E.E., Zhu, J., (ADNI), A.D.N.I.: Comparison of brain connectomes by mri and genomics and its implication in alzheimer's disease. BMC medicine **18**, 1–17 (2020)
24. Yeh, F.C.: Shape analysis of the human association pathways. Neuroimage **223**, 117329 (2020)
25. Yeh, F.C., Tseng, W.Y.I.: Ntu-90: a high angular resolution brain atlas constructed by q-space diffeomorphic reconstruction. Neuroimage **58**(1), 91–99 (2011)
26. Zhang, L., Wang, L., Gao, J., Risacher, S.L., Yan, J., Li, G., Liu, T., Zhu, D., Initiative, A.D.N., et al.: Deep fusion of brain structure-function in mild cognitive impairment. Medical image analysis **72**, 102082 (2021)
27. Zhang, L., Wang, L., Zhu, D., Initiative, A.D.N., et al.: Predicting brain structural network using functional connectivity. Medical image analysis **79**, 102463 (2022)
28. Zhu, D., Shen, D., Jiang, X., Liu, T.: Connectomics signature for characterizaton of mild cognitive impairment and schizophrenia. In: 2014 IEEE 11th International Symposium on Biomedical Imaging (ISBI). pp. 325–328. IEEE (2014)